Polymer-dispersed liquid-crystal coatings for ultrasound visualization: Experiment and theory

O. Trushkevych [1,*] V. Reshetnyak [2,3] M. Turvey [2] and R. S. Edwards [2]
[1]*School of Engineering, University of Warwick, Coventry, CV4 7AL, United Kingdom*
[2]*Department of Physics, University of Warwick, Coventry, CV4 7AL, United Kingdom*
[3]*Department of Physics, Taras Shevchenko National University of Kyiv, Kyiv, Ukraine*

(Received 5 December 2023; accepted 1 May 2024; published 5 June 2024)

Polymer dispersed liquid crystal (PDLC) films are formed of droplets of liquid crystal (LC) held in a polymer matrix. Similar to aligned LC films, PDLCs exhibit the acousto-optic (AO) effect when excited by acoustic waves of sufficient amplitude, whereby the PDLC film becomes transparent in the excited regions (acoustic clearing). Despite decades of research there is still debate over the mechanisms of the AO effect for the case of LC films, with several competing theories, and AO effects in PDLC have not been studied theoretically. This paper explores the AO effect in PDLC both experimentally and theoretically, and attempts a theoretical description of the observed phenomena based on the theoretical approach by Selinger *et al.* for aligned LC films. The acousto-optic effect in PDLC is shown to be due to direct interaction of acoustic waves with LC droplets, rather than due to compression of the droplet itself. Polarizing microscopy revealed changes in droplet shape at excited points. This is consistent with reorientation as a contributing factor, possibly coexisting with flows at higher excitation powers. In previous experimental studies PDLC films were prepared with cover slides, in the same way as LC AO cells, significantly limiting applications by adding complexity to the design. Also, to exhibit AO clearing it was considered that the PDLC needed to be prepared with high LC concentrations (over 75% by weight). We demonstrate that no cover slide is necessary, and that PDLC coatings without a cover have improved sensitivity to acoustic waves. We demonstrate the AO effect for LC concentrations as low as 40% by weight. The ability to use standard composition PDLC, with no top cover, is paving the way to paint-on visual ultrasound sensors.

DOI: 10.1103/PhysRevE.109.064701

I. INTRODUCTION

Fast visualization of ultrasound and vibration at ultrasound frequencies, using low cost large area passive sensing, would be highly attractive for a variety of applications, for example in nondestructive testing, transducer characterization, and condition monitoring. The gold-standard measurement for measuring such acoustic fields is laser doppler vibrometry, but this can be slow as measurement is done point-by-point. Fast visualization of ultrasound waves has previously been demonstrated using polymer dispersed liquid crystal (PDLC) films sandwiched between an ultrasound transducer and a glass cover, for PDLC films with high LC content (75% by weight) [1–4]. This gives clearing where the ultrasonic amplitude is sufficiently large, allowing visualization of vibrations. PDLC films are polymer films with encapsulated LC droplets [5,6]. The refractive indices of the polymer and LC are chosen to be mismatched when the LC is not aligned and the PDLC is in its ground state, scattering light and giving a milky appearance. When the LC is aligned by a field, it reorients and matches the refractive index of the matrix, turning the film transparent.

*o.trushkevych@warwick.ac.uk

The local preferred molecular orientation in a LC is called a director $\vec{n}$. There are two types of anchoring of molecules forming the LC phase on a polymer surface: planar ($\vec{n}$ tangential to the polymer surface) or homeotropic ($\vec{n}$ perpendicular to the polymer surface). Planar anchoring in LCs with positive dielectric anisotropy can produce two LC director distributions inside a droplet: bipolar and toroidal [7–9]. Bipolar configuration [Fig. 1(a)] is when the LC director is in one direction, with two topological boojum defects around the poles [7]. Toroidal alignment also has two defects but is harder to achieve [Fig. 1(b)] [9,10]. With homeotropic alignment, molecules in the droplet form a radial director profile, with a single hedgehog defect in the center [Fig. 1(c)].

Acoustic fields can affect the optical properties of LCs. Acousto-optic (AO) effects in aligned LC films have been extensively studied since the 1970s, predominantly in homeotropically aligned LC layers [11–21]. Interesting applications have been developed, including acoustography [12] (imaging of acoustic fields in a water bath using a LC cell held between crossed polarizers), and most recently a tuneable optical lens [22]. However, the exact mechanisms behind the AO effect in aligned LCs are still a matter of debate. There are three schools of thought suggesting different mechanisms and theoretical treatments:

(1) Reorientation through director-density coupling (developed for high frequencies and thick LC layers) [13,17,23,24].

(2) Acoustic streaming [14–16] (Couette and Poiseuille flows).

FIG. 1. Possible LC director configurations (director field lines) inside a droplet forming PDLC. (a) bipolar; (b) toroidal; (c) radial.

(3) Hyperelastic model with small anisotropic compressibility (reorientation through viscoelasticity) [25,26].

These have all been developed for aligned LCs, and the mechanisms in LC droplets that form PDLC are not understood.

Ultrasound can affect LC director orientation $\vec{n}$, but the suggested direction of reorientation is different in different works. In the nematic LC N-(4-Methoxybenzylidene)-4-butylaniline (MBBA), the reorientation was perpendicular to the direction of vibration [16,17] [see Fig. 2(a)]. Similar behavior was described in the proprietary LC used in acoustography [12] and theoretically described by Selinger *et al.* [13]. Harada *et al.* [22] used nematic LC RDP-85475. In their work an acoustic field reoriented the director parallel to the direction of vibration.

The LC material used in this work has planar anchoring on the polymer and forms bipolar droplets [Fig. 2(b)]. The direction of alignment of bipolar droplets is described by a bipolar axis and represented as a vector $\vec{L}$. In the unexcited state the orientation of the bipolar axes in neighbouring droplets is random, leading to light scattering. When an external electric field is applied, the direction of the bipolar axis in each droplet changes, with $\vec{L}$ aligning along the field for materials with positive dielectric anisotropy [7].

In previous studies on the AO effect in PDLC [1–4], as well as in all studies on the AO effect in aligned LC layers, LC and PDLC were produced such that they were sandwiched between two flat hard surfaces. For PDLC measurements, one surface was an ultrasound transducer and the other was a glass slide used as a top cover. The top cover is required for aligned LCs, and in PDLC it has previously been used as it may provide an interface with a step in acoustic impedance, a weight against which the LC droplets are deformed leading to reorientation, or a face against which viscous waves are formed [14,15]. However, PDLC films do not require a top cover for structural integrity or alignment, unlike aligned LC

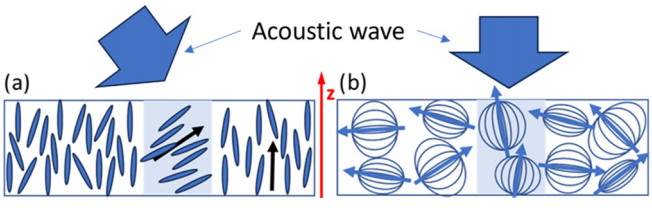

FIG. 2. Reorientation by acoustic fields. (a) reported experiments in homeotropically aligned nematic materials with negative dielectric anisotropy, the arrow represents orientation of LC director $\vec{n}$; (b) the suggested schematic of AO effect in PDLC in this work (E7 has positive dielectric anisotropy), curved lines in the droplets are director field lines; arrows indicate the orientation of the bipolar axis $\vec{L}$.) The orientation and angle of $\vec{L}$ is taken relative to axis z.

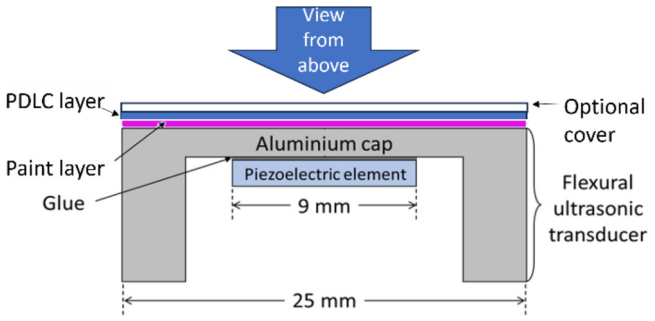

FIG. 3. Flexural transducer with PDLC layer.

films, and there is potential that one is not required to observe the AO effect. From an applications point of view, it would be beneficial to use PDLC as a thin, flexible and conformable film, paintlike, without the top cover, and hence it is important to explore whether it is possible to obtain the AO effect in paint-on PDLC films.

For ultrasound excitation above 2 MHz, as reported in Ref. [4], only small displacements, as low as several nm, were sufficient to cause clearing. While a definite conclusion about the mechanisms of acoustic clearing could not be reached in Ref. [4], the results supported the direct interaction of ultrasound with LC in droplets as the leading mechanism behind the observed effects. In this paper we present experimental and theoretical results, aiming to give a more definite answer regarding the nature of the AO effect in PDLC. We report experimental findings and address the two technical questions that are enabling for real world applications: the possibility of using paint-on PDLC coatings, including on nonflat surfaces, and the use of PDLC films with standard composition (50% polymer 50% LC). We discuss what the observed behavior means in terms of the mechanisms and develop a theory of the AO effect in PDLC. In this work, using typical nematic LC material E7, we observe behavior consistent with reorientation along the direction of vibration similar to behavior in optical lensing [22].

II. EXPERIMENTAL DETAILS

A flexural ultrasound transducer (RS instruments) with 25-mm diameter was used in this work, shown in Fig. 3 [3]. The transducer had a fundamental resonance around 40 kHz and produced higher-order modes with different excitation patterns when excited at higher frequencies [3,4]. The transducer was driven by a continuous sine wave using a function generator with a 25-W RF power amplifier. The high-order vibrational mode around 6.65 MHz was chosen due to its efficiency, recognizable appearance (smiley face due to variations in coupling between the piezoelectric element and vibrating cap) and sufficient resilience to changes in loading of the transducer. The excitation voltage was chosen to be sufficient to obtain clearing but not to overheat the sample. This was in the range of 1 V peak to peak, with a resulting power output into the transducer in the region of 1 W. The transducer heats up uniformly when operated at such powers, but stays below 45 °C. This is at least 15 °C below the temperature of transition into the isotropic phase for the nematic LC E7 used in this work.

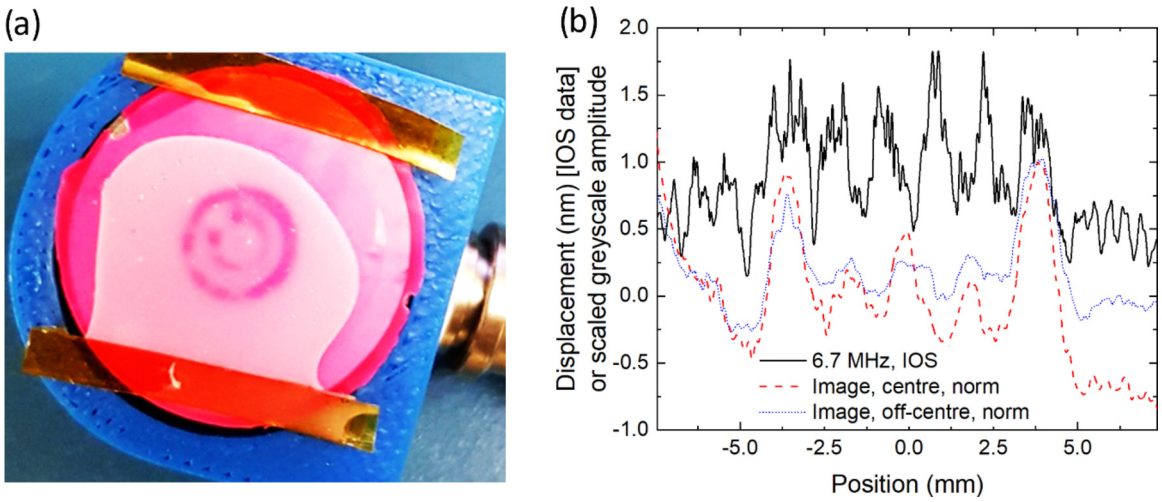

FIG. 4. Acousto-optic effect in PDLC film without glass cover, excitation at 6.65 MHz, film with 75% wt. LC composition. (b) interferometer line scan of the displacement of the transducer.

The transducer was coated with a thin layer of pink UV-curable varnish, to ensure good optical contrast when observing clearing. The PDLC films were produced in turns on the same transducer using a process described in Ref. [3]. In brief, liquid crystal E7 from Merck and UV curable Norland adhesive NOA68 were mixed at several concentrations of LC by weight (30%, 40%, 50% and 75% wt LC) using a magnetic stirrer at 60 °C, where the LC is in the isotropic phase. The 30% wt film did not scatter light due to the LC content being too low, and was not studied further. The LC-monomer mixture was drop-cast onto the cured varnish layer and covered with a top cover with spacers so that a 100-μm-thick film was formed. The top cover was a microscope slide attached to a thin transparent plastic film using ultrasound coupling gel, placed with plastic film facing the mixture. The samples were cured for 4 min. with UV intensity around 100 W/m^2. The chosen polymer does not stick well to the plastic film, so the top cover could be removed following the UV curing step, leaving a PDLC film with uniform thickness and no top cover.

The transducer-PDLC systems were studied using photography to capture AO effects on the macroscale, and with optical microscopy used in reflection mode (using bright field, polarized and circularly polarized modes of imaging) to study the effects on the microscale. While the LC is not chiral, the best contrast in reflection configuration was obtained using a circular polarized filter. Droplet size was under 10 μm in all films. Comparative measurement of the ultrasonic displacement of the transducer at the chosen frequency was made using an Intelligent Optical Systems two-wave mixer interferometer. A line-scan was made across the center-line of the transducer with the coatings removed, and displacement measured as a function of position. Calculations were then done to understand the behavior of the PDLC.

III. RESULTS AND DISCUSSION

A. Deformation of high concentration PDLC

The PDLC film at 75% composition was analyzed without a top cover. Figure 4(a) shows an image taken at 6.65 MHz, showing the mode vibrational pattern observed. Figure 4(b) shows the measurement of the transducer displacement for a resonant mode at 6.67 MHz once the films were removed (black line). Note that the resonant frequency will be shifted when the PDLC and paint layer are applied due to extra damping and weight on the sensor, and hence this mode will not be the exact same vibrational mode as imaged with the PDLC; there are closely spaced modes in this frequency region and it is complicated to find the exact same mode without full two-dimensional laser scanning. However, the mode will have similar behavior to the one tested using the PDLC, and can be compared for resolution. Figure 4(b) also includes analysis of the photograph of the PDLC for comparison. The image was converted to greyscale, then the greyscale values across a line across the center of the transducer (red) and just offset from the center (green) were taken. These were normalized and scaled so that they had similar values to the displacement measured in nm for comparison. The results show that the PDLC can resolve the mode vibration shape at this high frequency as the displacement correlates with the optical image. This confirms that the top cover is not required for observation of the AO effect in PDLC, with the image in fact obtained more efficiently than when a cover is used.

Optical microscopy in the bright field was conducted as voltage was applied to the transducer to understand the mechanism behind the AO effect and why it appears enhanced when the top cover is removed, contrary to earlier assumptions [1]. Figure 5(a) shows a photograph of the film for no ultrasonic excitation, where the surface of the film appears mostly flat. Images were taken away from pools of LC on the sample surface. Upon excitation, the surface appears apparently deformed [Fig. 5(b)], with dropletlike regions extending perpendicular to the transducer plane. The surface returned to the original state once the excitation was switched off. If the droplets were smaller anchored pools on the sample surface, they would have coalesced upon ultrasound excitation or with time as they were very close together, and LC has planar anchoring on the polymer and wets the surface well; we did not see this change. We speculate that the observation could be interpreted as LC droplets deforming as a result of LC director reorientation, as illustrated in Fig. 5(c), with the

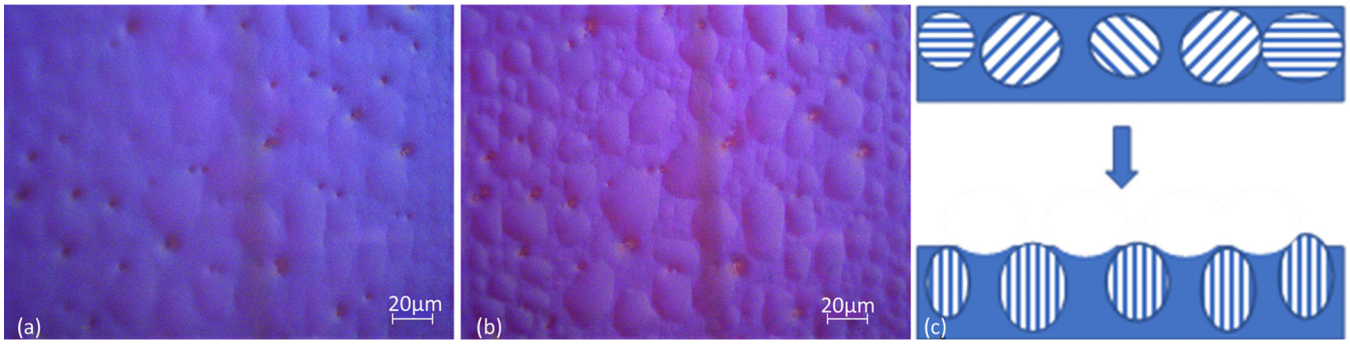

FIG. 5. Bright field optical microscopy in reflection on a thin PDLC film without top cover, the scale bar is 20 μm. (a) no excitation; (b) transducer on −ultrasound excitation; (c) suggested schematic of LC reorientation leading to the apparent change of droplet shape. The image was taken away from the area where large pools of LC were noticeable.

deformation via either director-density coupling or vertical flows. If a cover slide had been present, it would have suppressed the shape change and therefore opposed reorientation (and related change in the effective refractive index of the droplet), thus suppressing the AO effect. This might explain why the AO effect is clearer in this work without the cover slide. Supplemental Material [27] contains further observation of the deformation accompanying the excitation with acoustic field in PDLC with 75% wt LC content. The change in internal droplet geometry will be investigated further in later work.

For high LC content PDLC samples, such as the 75% wt PDLC film used here, a pool of LC can often be found on the top of the sample. Figure 6 shows a region of the surface where such a pool is found, for (a) no ultrasonic excitation, and (b) excitation at 6.7 MHz. Circularly polarized light gave the best contrast for imaging this phenomenon. Ultrasonic excitation induced stable and reproducible shapes that we identify as flow-induced rolls. The rolls had dimensions of the ultrasound wavelength ($\lambda = 223\,\mu$m at 6.7 MHz, calculated from the published value of speed of ultrasound in E7′s main component 5CB at 5–10 MHz [28]). The observed rolls are consistent with results reported in Ref. [15] for LCs, but cannot be supported in PDLC droplets that have size $\leqslant 40$ μm (Fig. 5). The droplet size distribution in a PDLC film of the same composition was shown to have the largest number of droplets $\leqslant 4$ μm [4].

B. PDLC films with LC content below 75%wt

In previous studies it was believed that only films with 75% wt. LC and higher exhibit the acousto-optic effect at achievable ultrasound levels [1–4]. However, all these studies were done using a top cover, which suppresses the effect. High LC content PDLC films are not practical for applications, as they are fragile and are not as effective in the scattering state due to low polymer content. This leads to lower contrast between opaque and clear, and the need to make films thicker to ensure sufficient scattering. The amount of LC required further drives the cost up.

Figure 7 shows images taken for the 6.65-MHz excitation for an input voltage to the amplifier of 900 mV, for (a) 50% wt LC, and (b) 40% wt LC, without the top cover. These films were prepared in the same manner as for the 75% wt PDLC film, and the mode image is still clear. These concentrations are typical in commercial PDLC films used for privacy windows. Figure 7(c) shows a 50% wt LC film prepared using a different method; the film was prepared directly onto a thin plastic sheet (around 100 μm thickness), producing a removable sensor, and the film was coupled to a different transducer using ultrasound gel. There is some variability in transducers within the same batch which becomes noticeable at higher frequencies, and the coupling and damping conditions are different to the films produced directly on the transducer. However, an image of the mode is again clearly produced,

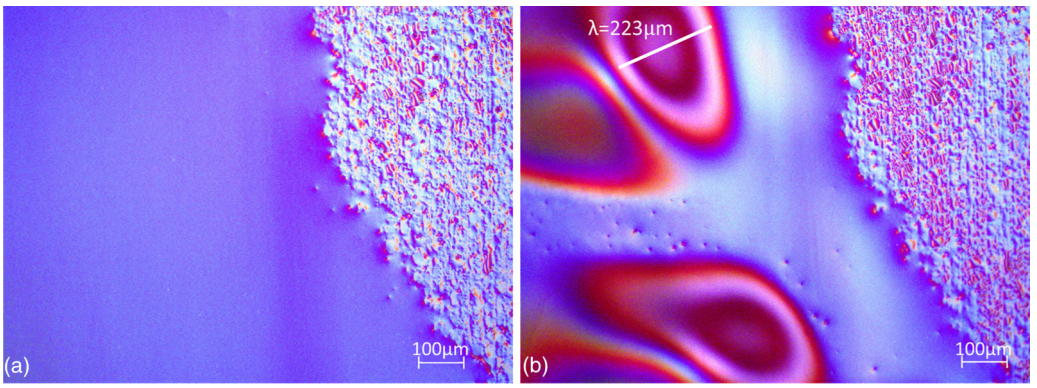

FIG. 6. The surface of a PDLC film with a pool of unconstrained LC on the left side in circularly polarized light. (a) no excitation and (b) with ultrasound excitation. Ultrasound excitation at 6.7 MHz leads to establishment of stable rolls. The size of rolls is consistent with ultrasound wavelength, indicated on the figure. The scale bar is 100 μm.

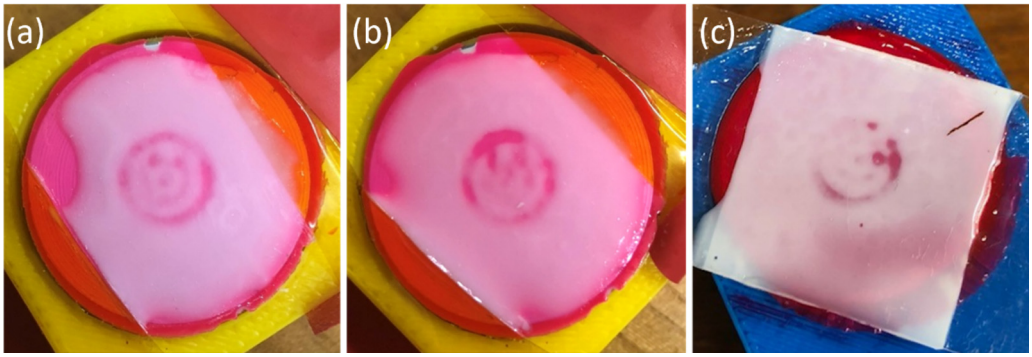

FIG. 7. PDLC coatings on top of transducer, excited at 6.65 MHz and 900 mV to amplifier, (a) 50% wt LC; (b) 40% wt LC. (c) a removable PDLC prepared between two plastic sheets, coupled using ultrasound gel to transducer, 50% wt. LC, same excitation conditions.

showing that PDLC films could be used both as paint-on or removable film sensors.

The photographs for the same mode but different LC concentrations [Figs. 4(a), 7(a), and 7(b)] were compared to analyze the clearing. Firstly, the images were converted to grayscale. Three points were chosen on each photograph, in similar positions:

(1) The uncleared area (white reference).

(2) Area not covered by the PDLC film (background/transparent reference).

(3) Cleared area (measured transparency value).

The values of the grayscale (out of 256) were recorded at each chosen position and used to calculate contrast as a percentage, with 0% being white (no clearing) and 100% being transparent (fully cleared), for the same transducer settings. Table I summarizes the findings, showing that contrast is similar for all concentrations. Films with standard composition can therefore be used in place of high concentrations.

C. Theoretical model of AO effect in PDLC

The observations presented above point to reorientation as being the leading mechanism behind the AO effect. Figure 2(a) summarizes the behavior reported previously for homeotropically aligned nematic materials, with the black arrow showing the LC director $\vec{n}$. Based on the measurements taken of E7 in PDLC, the suggested AO effect is shown in Fig. 2(b). In this section a theoretical model is presented to describe the effective refractive index change due to the influence of ultrasound. The model assumes that the LC droplets are bipolar with some initial distribution of the bipolar axis orientation, and that the leading mechanism is reorientation. We do not include the change in droplet shape in this model as this would significantly complicate the system.

The interaction of the LC director $\vec{n}$ with ultrasound is modeled within the approach suggested by Selinger and coworkers [13], with the volume density of the interaction between the LC and ultrasound wave F_{us} given by

$$F_{us} = \frac{u_2 \rho_0}{v^3} I_0 k^2 (\vec{n} \cdot \vec{e})^2 \equiv \alpha I_0 (\vec{n} \cdot \vec{e})^2, \tag{1}$$

where k is the ultrasound wave vector, $\vec{e}$ is the ultrasound wave polarization vector (displacement vector), u_2 is a parameter describing the magnitude of the interaction (strength of the coupling between the director and density gradients), I_0 is the sound intensity, v is the sound velocity, and ρ_0 is the LC density. This energy of the interaction is averaged over the ultrasound wave oscillations. For PDLC, when ultrasound is applied both the LC director inside each droplet and the droplet bipolar axis can be reoriented [29]. The LC director reorientation is generally a nonlinear function of the sound intensity. At low sound intensity, the reorientation can be assumed to be proportional to I_0; while at high intensity the director is aligned perpendicular to the wave vector, as observed in our experiments and in contrast to [13], and the LC director reorientation saturates.

Following previous work [30], we assume that an individual droplet is spherical and has an initial bipolar axis $\vec{L}_0$. This initial ground state is likely prescribed by small irregularities in droplet shape and surface anchoring. There is an elastic energy associated with rotation about this axis, F_{el}. We propose that the LC interaction with the polymer matrix has a simple phenomenological form,

$$F_{el} = -\pi W R^2 (\vec{L} \cdot \vec{L}_0)^2, \tag{2}$$

where the parameter $W > 0$ characterizes the magnitude of the interaction related to anchoring, and R is the droplet radius. The LC interaction with the polymer matrix is assumed to be proportional to R^2 because it occurs at the droplet boundary, and is therefore likely to scale with the droplet surface area.

At low ultrasound intensity the director configuration inside a droplet remains unchanged, but the applied ultrasound may reorient both the LC director inside the droplet and the bipolar axis of the droplet to a new direction $\vec{L}$ [shown schematically in Fig. 2(b)] [31]. The initial and final axes of the droplets are described by distribution function p.

Within a particular droplet, the distribution of directors is nonuniform. One may describe this nonuniformity in terms of

TABLE I. Contrast in PDLC films with no top cover.

Film	75% wt LC	50% wt LC	40% wt LC
Contrast	85%	72%	87%

a droplet order parameter S,

$$S = \left\langle \left(\tfrac{3}{2}(\vec{n}\cdot\vec{L})^2 - \tfrac{1}{2}\right)\right\rangle, \tag{3}$$

where the averaging is within the droplet volume. If the director field lines within the droplet are surface contours of ellipsoids, $S = 0.818$ [30]. Then the perpendicular component $\tilde{\varepsilon}_\perp$ and anisotropy $\tilde{\varepsilon}_a = \tilde{\varepsilon}_{||} - \tilde{\varepsilon}_\perp$ of the bipolar droplet effective dielectric tensor $\tilde{\varepsilon}$ at optical frequency becomes

$$\tilde{\varepsilon}_\perp = \varepsilon_\perp + \tfrac{1}{3}(1-S)\varepsilon_a, \tag{4}$$

$$\tilde{\varepsilon}_a = S\varepsilon_a, \tag{5}$$

where $\varepsilon_\perp$ and ε_a are perpendicular and anisotropy components of the LC dielectric tensor. These values are required when describing the optical properties, e.g., birefringence and light scattering. To characterize the increasing alignment of the droplets' bipolar axes under the applied sound field, it is convenient to use the bipolar axis order parameter Q [30],

$$Q = \int_0^{\pi/2} \left(\frac{3}{2}\cos^2\theta - \frac{1}{2}\right) p(\theta, I_0)\sin\theta d\theta, \tag{6}$$

where θ is the angle between $\vec{L}$ and the z axis. For randomly distributed bipolar axes, $Q = 0$ (PDLC film in the OFF state, no ultrasound applied); at sufficiently high ultrasound intensity, Q approaches unity because the bipolar axes all become aligned in one direction along the displacement vector. The bipolar order parameter Q depends on the intensity of the sound applied to the PDLC film and the droplets' anchoring with the polymer matrix. It is convenient to introduce the nondimensional parameter ζ, which is related to the applied sound intensity as

$$\zeta = \left(\frac{R^2}{6\pi W}\right)^{1/2} \alpha I_0. \tag{7}$$

Combining Eqs. (1) and (2) we obtain the free energy for a single droplet

$$F = \alpha I_0 \int (\vec{n}\cdot\vec{e})^2 dV - \pi W R^2 (\vec{L}\cdot\vec{L}_0)^2, \tag{8}$$

where the integration is taken over the droplet volume. To rewrite Eq. (8) in terms of the bipolar axis $\vec{L}$ we present the LC director inside the droplet in the form $\vec{n} = (\vec{n}\cdot\vec{L})\vec{L} + \delta\vec{n}$, where the vector $\delta\vec{n}$ is uniformly distributed within the plane perpendicular to the bipolar axis $\vec{L}$. Then

$$\begin{aligned}\int (\vec{n}\cdot\vec{e})^2 dV &= \int (((\vec{n}\cdot\vec{L})\vec{L} + \delta\vec{n})\cdot\vec{e})^2 dV \\ &= \int ((\vec{n}\cdot\vec{L})(\vec{L}\cdot\vec{e}) + (\delta\vec{n}\cdot\vec{e}))^2 dV \\ &= (\vec{L}\cdot\vec{e})^2 \int (\vec{n}\cdot\vec{L})^2 dV + 2(\vec{L}\cdot\vec{e}) \\ &\quad \times \int (\vec{n}\cdot\vec{L})(\delta\vec{n}\cdot\vec{e}) dV + \int (\delta\vec{n}\cdot\vec{e})^2 dV. \end{aligned} \tag{9}$$

The second term here is zero, since $\delta\vec{n}$ is uniformly distributed, while the third term is independent of the bipolar axis direction, but might depend on the droplet order parameter. Finally we have

$$\begin{aligned} F &= \alpha I_0 \tfrac{2}{3}(S+0.5)(\vec{L}\cdot\vec{e})^2 - \pi W R^2 (\vec{L}\cdot\vec{L}_0)^2 \\ &\equiv \tilde{\alpha} I_0 (\vec{L}\cdot\vec{e})^2 - \pi W R^2 (\vec{L}\cdot\vec{L}_0)^2. \end{aligned} \tag{10}$$

The initial bipolar droplet orientation is given by the angle θ_0 with respect to the PDLC film normal (z axis). The ultrasound displacement is along the z axis, hence the free energy for a single droplet is given by

$$F = \tilde{\alpha} I_0 \cos^2\theta - \pi W R^2 \cos^2(\theta - \theta_0). \tag{11}$$

Now we average expression (11) with the bipolar axes distribution function to obtain

$$F_{av} = \int (\tilde{\alpha} I_0 \cos^2\theta - \pi W R^2 \cos^2(\theta - \theta_0)) p(\theta) d\cos\theta. \tag{12}$$

We assume that the droplets with their orientation Ω_0 (given by the angles θ_0, φ_0) within the solid angle $d\Omega_0$ are reoriented to the angles Ω within the solid angle $d\Omega$, therefore $\mathrm{p}(\theta,\varphi)d\Omega = \mathrm{p}(\theta_0,\varphi_0), d\Omega_0$. As $d\Omega = \sin\theta d\theta d\varphi = -d\,cos\theta d\varphi$.

We further assume that the distribution function does not depend on the angle φ. The ultrasound waves only change the angle θ_0, so we use the relation $p(\theta)d\cos\theta = p(\theta_0)d\cos\theta_0$ to obtain

$$F_{av} = \int (\tilde{\alpha} I_0 \cos^2\theta - \pi W R^2 \cos^2(\theta - \theta_0)) p(\theta_0) d\cos\theta_0. \tag{13}$$

Minimization of this function results in the following equation:

$$\tilde{\alpha} I_0 \sin 2\theta - \pi W R^2 \sin 2(\theta - \theta_0) = 0, \tag{14}$$

or

$$\theta = \tan^{-1} \frac{\sin 2\theta_0}{\tilde{\zeta}^2 + \cos(2\theta_0) + (\tilde{\zeta}^4 + 2\tilde{\zeta}^2 \cos 2\theta_0 + 1)^{1/2}}, \tag{15}$$

where $\tilde{\zeta} = \frac{2}{3}\left(\frac{R^2}{6\pi W}\right)^{1/2} \alpha (S+0.5) I_0$.

Having found the bipolar axes reorientation angle subject to different initial orientation one can calculate the bipolar axis order parameter Q, using Eq. (15) for $\theta(\theta_0, \tilde{\zeta})$ and changing the integration over θ by the integration over θ_0 as above.

$$\begin{aligned} Q &= \left\langle \frac{1}{2}(3\cos^2\theta - 1)\right\rangle_{\text{droplets}} \\ &= \frac{1}{2}\int_0^{\pi/2} (3\cos^2\theta - 1) p(\theta) d\cos(\theta). \end{aligned} \tag{16}$$

In Fig. 8 the bipolar axis order parameter is plotted vs the nondimensional parameter $\tilde{\zeta}$ (nondimensional ultrasound intensity) and overlayed with the experimental result of transmisisson through the PDLC film as a function of acoustic intensity. The transmission of the PDLC film should depend on the bipolar axis order parameter Q. However, this dependence is not expected to be linear. In Fig. 8 when we superimpose $\mathrm{Q}(\tilde{\zeta})$ (right axis) and T(I), surprisingly the dependences are rather similar, that suggests that the main contribution of the bipolar order parameter Q in the transmission T comes from the linear term, $\mathrm{T} \sim \mathrm{Q}$. Furthermore, from Fig. 8 and the definition of $\tilde{\zeta}$, one can deduce that with

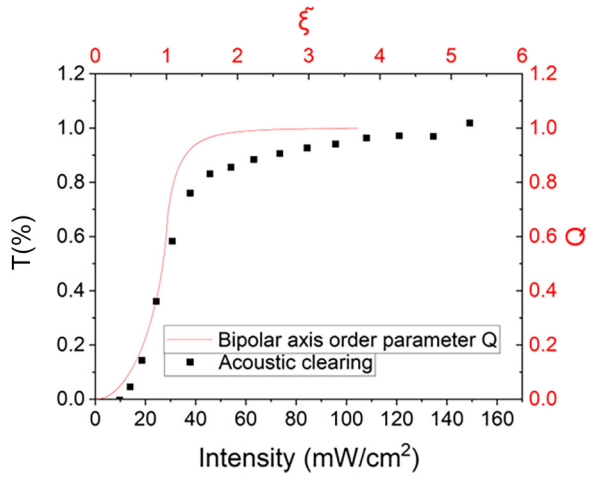

FIG. 8. The bipolar axis order parameter vs nondimensional parameter $\tilde{\xi}$ (nondimensional ultrasound intensity), solid line, and the experimental measurement of clearing (transmission) as a function of ultrasound intensity (squares).

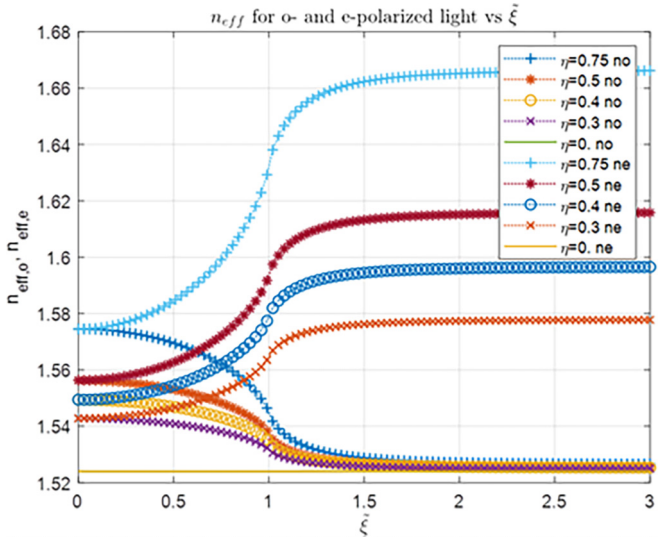

FIG. 9. Ordinary n_0 and extraordinary n_e refraction indices of LC droplets in PDLC film vs parameter $\tilde{\xi}$ for different volume fractions of LC.

the same ultrasound intensity a higher level of reorientation will be achieved in films with larger droplets and with lower anchoring strength W.

The bipolar axis order parameter can then be related to the optical properties of the PDLC. The full expression describing scattering characteristics is beyond the scope of this paper, here we will briefly outline the refractive indices of the droplets as a result of ultrasound excitation. The simplest approximation to the effective dielectric tensor of a PDLC film at optical frequencies would be

$$\varepsilon_{ij}^{\mathrm{PDLC}} = \varepsilon_p(1-\eta)\delta_{ij} + \eta(\tilde{\varepsilon}_\perp \delta_{ij} + \tilde{\varepsilon}_a \langle L_i L_j \rangle_{\mathrm{droplets}}), \quad (17)$$

where ε_p is the dielectric permittivity of the polymer, which is assumed to be isotropic, and η is the volume fraction of LC in the film. Rewriting Eq. (17) in terms of the bipolar axis order parameter gives

$$\begin{aligned} \varepsilon_\perp^{\mathrm{PDLC}} &= \varepsilon_p(1-\eta) + \eta\left(\tilde{\varepsilon}_\perp + \tilde{\varepsilon}_a \tfrac{1}{3}(1-Q)\right) \equiv n_0^2, \\ \varepsilon_{||}^{\mathrm{PDLC}} &= \varepsilon_p(1-\eta) + \eta\left(\tilde{\varepsilon}_\perp + \tilde{\varepsilon}_a \tfrac{2}{3}\left(\tfrac{1}{2}+Q\right)\right) \equiv n_e^2. \end{aligned} \quad (18)$$

This can then be converted to refractive index to explain the observed optical properties of the films. Figure 9 shows the ordinary and extraordinary refractive indices of PDLC film vs. parameter $\tilde{\xi}$ for different volume fractions of LC (given in the legend; $\eta = 0.4$ corresponds to 40% wt LC, etc.). The refractive indexes in films with 40% and 50% wt LC content (red stars and blue and yellow open circles in Fig. 9) are similar, supporting the experimental observations that these films perform at a similar level.

D. Combining theory and experiment

The volume part of the free energy for the case of PDLC switching by electric field has been described in Refs. [8] and [30] as

$$F_{\ \mathrm{electric}} = \varepsilon_a(\vec{n}\cdot\vec{E})^2 \sim V^2. \quad (19)$$

The volume part of the free energy for the case of PDLC switching by ultrasound can be similarly described as

$$F_{\ \mathrm{ultrasound}} = \alpha I_0(\vec{L}\cdot\vec{e})^2 \sim I_0. \quad (20)$$

Thus, one may expect similar transmittance plots when switching PDLC with voltage V and with ultrasound when plotting acoustic clearing as functions of V^2 and intensity I_0, [13]. Note that depending on the sign of the parameter α, the LC director should reorient either perpendicular or parallel

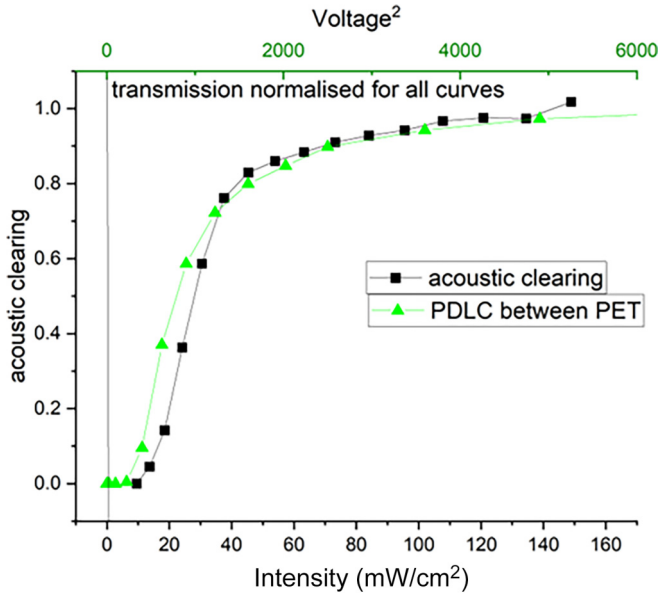

FIG. 10. Experimental data comparison of switching PDLC film (E7 and NOA65) transmittance by voltage and ultrasound. Transmittance of PDLC as a function of voltage squared uses data taken from Nasir *et al.* [32] (green triangles), while black squares show acoustic clearing.

to the direction of the displacement. In our case L is in the direction of displacement.

Figure 10 shows measurement of the acoustic clearing using analysis of the greyscale of photographs of the clearing, as described above, for clearing using acoustic or electric fields. The electro-optic effect data was taken from Nasir *et al.* [30], for PDLC (E7 and NOA65) laminated between two polyethylene terephthalate slides. The optical switching behavior by the electric field is very similar to that by acoustic field, as expected, and similar behavior to that predicted in Fig. 8 is produced.

IV. CONCLUSIONS

We have demonstrated the acousto-optic effect in paint-on and removable PDLC films with LC content as low as 40% wt, offering low cost and potentially fast large area ultrasound visualization. The mechanisms behind the observed acousto-optic effect are mostly reorientation, confirmed using polarized optical microscopy, however, acoustic streaming may contribute in other systems where ultrasound wavelength is comparable to droplet size. Rayleigh-Bernard convection flows could be a small additional contributor to the observed acousto-optic effect.

A theory of the acousto-optic effect in PDLC droplets has then been described through the reorientation mechanism, based on the director-density coupling theory developed by Selinger *et al.* for aligned LC films [13]. The reorientation direction was opposite to that described in Ref. [13] due to the different LC material used. The theoretical description matches experimental data.

Based on the achieved understanding of the acousto-optic effect in PDLC films as being primarily due to reorientation and flows, we hypothesize that

(1) To obtain films with higher sensitivity, PDLC films with larger droplets, and LC-polymer combinations with lower anchoring strength, should be used to facilitate reorientation. The size of droplet will be limited by the maximum size which will give optical scattering in the unaligned state.

(2) To obtain a less steep response to excitation and allow greyscale imaging of the intensity of the detected ultrasound, a sample with large polydispersity (different droplet sizes) and with droplets of different elongations in different directions could be used. This will give reorientation and flows over a broad range of power levels in nieghboring positions on the film. These predictions will be tested in further research.

ACKNOWLEDGMENTS

Part of this work was supported by EPSRC grant EP/L022125/1, and by funding from the University of Warwick's Energy and Materials Global Research Priority networks. V.R. is supported by an IAS Fernandes Fellowship and the University of Warwick. M.T. thanks FIND-CDT (EPSRC EP/S023275/1) for funding her PhD.

[1] Y. J. Liu, X. Ding, S.-C. S. Lin, J. Shi, I.-K. Chiang, and T. J. Huang, Surface acoustic wave driven light shutters usingpolymer-dispersed liquid crystals, Adv. Mater. **23**, 1656 (2011).

[2] Y. J. Liu, M. Lu, X. Ding, E. S. P. Leong, S. Lin, J. Shi, J. H. Teng, L. Want, T. J. Bunning, and T. J. Huang, Holographically formed, acoustically switchable gratings based on polymer-dispersed liquid crystals, J. Lab. Autom. **18**, 291 (2013).

[3] O. Trushkevych, T. J. R. Eriksson, S. N. Ramadas, S. Dixon, and R. S. Edwards, Acousto-optics with polymer dispersed liquid crystals for ultrasound sensing, Appl. Phys. Lett. **107**, 054102 (2015).

[4] R. S. Edwards, J. Ward, L. Zhou, and O. Trushkevych, The interaction of polymer dispersed liquid crystal sensors with ultrasound, Appl. Phys. Lett. **116**, 044104 (2020).

[5] J. W. Doane, N. A. Vaz, B. Wu, and S. Žumer, Field controlled light scattering from nematic microdroplets, Appl. Phys. Lett. **48**, 269 (1986).

[6] D. Coates, Polymer-dispersed liquid crystals, J. Mater. Chem. **5**, 2063 (1995).

[7] H.-S. Kitzerow, Polymer-dispersed liquid crystals From the nematic curvilinear aligned phase to ferroelectric films, Liq. Cryst. **16**, 1 (1994).

[8] D.-K. Yang and S.-T. Wu, *Fundamentals of Liquid Crystal Devices*, 2nd ed. (Wiley, Chichester, UK, 2015).

[9] G. H. Springer and D. A. Higgins, Toroidal droplet formation in polymer-dispersed liquid crystal films, J. Am. Chem. Soc. **122**, 6801 (2000).

[10] J. Jiang and D.-K. Yang, Bipolar to toroidal configuration transition in liquid crystal droplets, Liq. Cryst. **45**, 102 (2018).

[11] H. Mailer, K. L. Likins, T. R. Taylor, and J. L. Fergason, Effect of ultrasound on a nematic liquid crystal, Appl. Phys. Lett. **18**, 105 (1971).

[12] J. S. Sandhu, H. Wang, and W. J. Popek, Acoustography for rapid ultrasonic inspection of composites, *Proceedings SPIE*, Nondestructive Evaluation of Materials and Composites **2944**, 1117 (1996).

[13] J. V. Selinger, M. S. Spector, V. A. Greanya, B. T. Weslowski, D. K. Shenoy, and R. Shashidhar, Acoustic realignment of nematic liquid crystals, Phys. Rev. E **66**, 051708 (2002).

[14] O. A. Kapustina, E. H. Kozhevnikov, and G. N. Yakovenko, Optical properties of homotropically oriented nematic-crystal elliptically deformed nematic crystal layer, Zh. Exp. Teor. Fiz. **87**, 849 (1984) [Sov. Phys. JETP **60**, 483 (1984)].

[15] O. A. Kapustina, Ultrasound-initiated structural transformations in liquid crystals (A review), Phys. Acoust. **54**, 180 (2008).

[16] O. A. Kapustina, Liquid crystal acoustics: A modern view of the problem, Crystallogr. Rep. **49**, 680 (2004).

[17] J. L. Dion and A. D. Jacob, A new hypothesis on ultrasonic interaction with nematic liquid crystal, Appl. Phys. Lett. **31**, 490 (1977).

[18] L. E. Davis and J. Chambers, Optical scattering in a nematic liquid crystal induced by acoustic surface waves, Electron. Lett **7**, 287 (1971).

[19] K. Miyano and Y. R. Shen, Domain pattern excited by surface acoustic waves in a nematic film, Appl. Phys. Lett. **28**, 473 (1976).

[20] F. M. Leslie, An analysis of a flow instability in nematic liquid crystals, J. Phys. D **9**, 925 (1976).
[21] Y. Kagawa, T. Hatakeyama, and Y. Tanaka, Vibro-optical and vibro-dielectric effect in nematic liquid crystal layer, J. Sound Vib. **41**, 1 (1975).
[22] Y. Harada, D. Koyama, M. Fukui, A. Emoto, K. Nakamura, and M. Matsukawa, Molecular orientation in a variable-focus liquid crystal lens induced by ultrasound vibration, Sci. Rep. **10**, 6168 (2022).
[23] A. P. Malanoski, V. A. Greanya, B. T. Weslowski, M. S. Spector, J. V. Selinger, and R. Shashidhar, Theory of the acoustic realignment of nematic liquid crystals, Phys. Rev. E **69**, 021705 (2004).
[24] V. A. Greanya, A. P. Malanoski, B. T. Weslowski, M. S. Spector, and J. V. Selinger, Dynamics of the acousto-optic effect in a nematic liquid crystal, Liq. Cryst. **32**, 933 (2005).
[25] P. Biscari, A. DiCarlo, and S. S. Turzi, Anisotropic wave propagation in nematic liquid crystals, Soft Matter **10**, 8296 (2014).
[26] S. S. Turzi, Viscoelastic nematodynamics, Phys. Rev. E **94**, 062705 (2016).
[27] See Supplemental Material at http://link.aps.org/supplemental/10.1103/PhysRevE.109.064701 for a change in PDLC film profile on semi-convex lens when excited with ultrasound and comparison of mechanisms contributing to acousto-optic effect and glass cover role.
[28] A. V. Glushchenko, V. S. Sperkach, and O. V. Yaroshchuk, Sound propagation in liquid crystal 5CB and 5CB based aerosil suspensions, Int. J. Fluid Mech. Res. **30**, 299 (2003).
[29] S. C. Jian and D. K. Rout, Electro-optic response of polymer dispersed liquid-crystal films, J. Appl. Phys. **70**, 6988 (1991).
[30] V. Y. Reshetnyak, T. J. Sluckin, and S. J. Cox, Effective medium theory of polymer dispersed liquid crystal droplet systems: II. Partially oriented bipolar droplets, J. Phys. D **30**, 3253 (1997).
[31] B. G. Wu, J. H. Erdmann, and J. W. Doane, Response times and voltages for PDLC light shutters, Liq. Cryst. **5**, 1453 (1989).
[32] N. Nasir, H. Hong, M. A. Rehman, S. Kumara, and Y. Seo, Polymer-dispersed liquid-crystal-based switchable glazing fabricated via vacuum glass coupling, RSC Adv. **10**, 32225 (2020).